Dental Materials Journal 2011; 30(3): 286–292

Phase transformation of zirconia ceramics by hydrothermal degradation

Yohei KAWAI[1], Motohiro UO[1], Yongming WANG[2], Sayaka KONO[1], Somei OHNUKI[2], and Fumio WATARI[1]

[1]Department of Biomedical Materials and Engineering, Graduate School of Dental Medicine, Hokkaido University, Kita 13 Nishi 7, Kita-ku, Sapporo 060-8586, Japan

[2]Division of Material Science, Graduate School of Engineering, Hokkaido University, Kita 13 Nishi 7, Kita-ku, Sapporo 060-8586, Japan

ABSTRACT

Zirconia has found wide application in dentistry because of its high mechanical strength and superior esthetic properties. However, zirconia degradation caused by phase transformation occurring in a hydrothermal environment is of concern. In the present study, phase transformation and microstructure of tetragonal zirconia polycrystal partially stabilized with yttrium oxide (Y-TZP) and alumina-toughened zirconia (ATZ) sintered at different temperatures were estimated. On grazing angle X-ray diffraction analysis, ATZ showed less phase transformation to the monoclinic phase during hydrothermal treatment and this transformation appeared to occur within a few micrometers below the surface. At a higher sintering temperature the monoclinic phase content of ATZ was found to be lesser than that of Y-TZP, indicating that the alumina in ATZ was effective in suppressing hydrothermal degradation. Examination by transmission electron microscopy and studying of electron backscatter diffraction patterns indicated that grain growth in ATZ was slightly suppressed compared with that in Y-TZP at higher sintering temperatures. The present study demonstrated the effect of adding alumina to zirconia for suppressing hydrothermal degradation and studied the effect of this addition on grain growth in zirconia.

Keywords: Zirconia, Phase transformation, Hydrothermal degradation

INTRODUCTION

Zirconia has been one of the most important ceramic materials for well over a century and the discovery of a mechanism for transformational toughening of zirconia to resist crack propagation in 1975 resulted in improvement of its mechanical properties[1,2]. Since then, zirconia has been used for wear applications, thermal barrier coatings, optical fiber connectors, and most recently, for biomedical applications because of its improved performance[3,4]. The use of zirconia ceramics in dental restorations (e.g., framework of fixed partial dentures and dental implants) has increased because of their high mechanical toughness, superior esthetic properties, and biocompatibility[5]. In the early 1990s, tetragonal zirconia polycrystal partially stabilized with yttrium oxide (Y-TZP) was introduced to dentistry for use as a core material for all-ceramic restorations and was made available through the CAD/CAM technique. As a result of transformation toughening during manufacture, Y-TZP displays superior mechanical properties compared with other all-ceramic systems[6,7]. For example, a flexural strength of 900–1200 MPa was recorded for Y-TZP in vitro, which is higher than the flexural strength for other dental alloys[7].

Despite the success of zirconia and its variegated applications, it has now become apparent that zirconia ceramics also have a drawback, in that they have a propensity to undergo low-temperature degradation (LTD) in the presence of moisture[8-13]. This is a kinetic phenomenon in which the polycrystalline tetragonal material slowly transforms into monoclinic zirconia over a rather narrow but important temperature range, typically between room temperature and approximately 400°C, depending on the stabilizer used, its concentration, and the grain size of the ceramic. This phase transformation is followed by microcracking and loss of strength[11-13]. In the application of zirconia to dental restorations, there is concern about its degradation when constantly used in a humid atmosphere at body temperature over a long period of time and when it is autoclaved for sterilization.

Alumina-toughened zirconia (ATZ) was thus developed to further improve the mechanical properties of zirconia. This material combined the hardness and wear resistance of alumina with the fracture toughness and bending strength of zirconia[14,15]. Further, the addition of alumina helped suppress the propagation of phase transformation into the bulk of the material and increased the hydrothermal stability of the tetragonal phase[14,16]. Ban et al. suggested that there were no changes in fracture toughness of ATZ after autoclaving, but the conventional Y-TZP showed a slight decreasing after autoclaving[11].

When the degradation of Y-TZP and ATZ was compared in a hydrothermal environment, ATZ exhibited a lower phase transformation rate compared with Y-TZP and a decelerated aging progress in a hydrothermal environment at body temperature after 50 years *in vivo*[9,16]. Thus, ATZ showed better mechanical properties and good durability with respect to LTD; however, the reason for the high LTD durability of ATZ is not known.

In the present study, phase transformation of Y-TZP and ATZ sintered at different temperatures was estimated using grazing angle X-ray diffraction (XRD) analysis after hydrothermal treatment, and the surfaces were examined by transmission electron microscopy (TEM) and by studying the electron backscatter diffraction pattern (EBSP).

MATERIALS AND METHODS

Preparation of zirconia substrate

Two kinds of zirconia ceramics (Y-TZP and ATZ) were used in the present study, as shown in Table 1. The typical SEM images of both powders were shown in Fig.1. The diameter of zirconia powders were estimated 57.0±21.2 μm forY-TZP and 51.4±10.6 μm for ATZ from SEM observations.

Table 1. Materials used in the present study

Code	Manufacturer	Product Name	Composition
Y-TZP	Daiichi Kigenso Kagaku Kogyo	HSY-3FSD	94.4wt% ZrO_2 5.6wt%Y_2O_3
ATZ	Daiichi Kigenso Kagaku Kogyo	ATZ-80SD(D)	75.2wt% ZrO_2 4.5wt% Y_2O_3 20.3wt% Al_2O_3

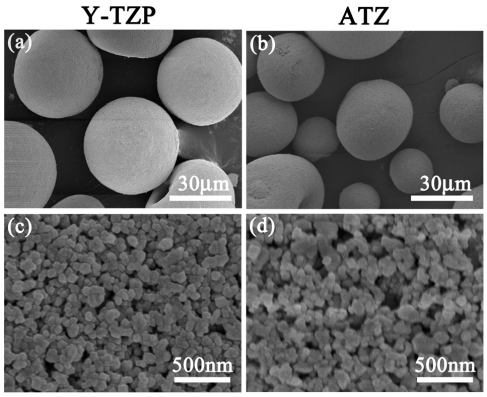

Fig. 1 The typical SEM images of Y-TZP powders at (a) lower and (c) higher magnification and ATZ powders at (b) lower and (d) higher magnification.

Both powders consisted of the primary particles, which diameter was approximately 30 nm. Y-TZP and ATZ powders (0.6 g) were pressed into a disk shape using a cylindrical mold measuring 10 mm in diameter, and sintered at 1350°C, 1400°C, and 1450°C for 2 h in air. The sintered zirconia disks were polished with emery paper (#2000), 1 μm alumina suspension, and colloidal silica suspension, and cleaned by sonication. Polished specimens were then autoclaved in distilled water (DW), Hanks' solution (Hanks), and lactic acid solution at 140°C, 2 atm for 3, 7, and 14 days.

XRD analyses

The crystal phase of the autoclaved specimen surfaces was analyzed with an X-ray diffractometer (XRD, Rigaku, Multiflex, Tokyo, Japan) using the conventional 2θ–θ method and the grazing angle method (incident angle θ = 1° and 2°). XRD analysis was performed using Cu Kα radiation at 40 kV and 30 mA. Diffractograms were obtained from 25° to 36° at a scan speed of 0.5°/min. The depth of grazing angle XRD could be varied by changing the incident angle of the X-ray. The penetration depth of grazing angle XRD, x, was derived as follows[17]:

$$x = -\ln(1 - Gx)/[\mu(\mathrm{cosec}\,\alpha + \mathrm{cosec}\,\beta)] \quad (1)$$

$$\beta = 2\theta - \alpha \quad (2)$$

where Gx, μ, and α represent the relative diffracted X-ray intensity up to depth x, the linear absorption coefficient, and the incidence angle, respectively[17]. The penetration depth of the incident and diffracted X-rays when Gx = 0.99 with incidence angle of 1° and 2° were estimated as 1.2 and 2.3 μm, respectively. Thus, XRD analysis within a few micrometers of the surface could be performed using grazing angle XRD by changing the incident angle.

The monoclinic zirconia content, Vm, was derived using Toraya's equations[18]:

$$Vm = 1.311Xm/(1 + 0.311Xm) \quad (3)$$

$$Xm = [Im_{(-111)} + Im_{(111)}]/[Im_{(-111)} + Im_{(111)} + It_{(101)}] \quad (4)$$

where Xm is the integrated intensity ratio, and It and Im represent the integrated intensity of the tetragonal (101) and monoclinic [(111) and (−111)] peaks around 30°, 31°, and 28°, respectively.

TEM and EBSP analyses

Microstructural observations of the specimens were carried out by TEM (JEM-2010; JEOL, Tokyo, Japan), operated at an acceleration voltage of 200 kV. An argon-ion milling apparatus (EIS-9100; JEOL) was used to prepare the TEM specimen in order to reduce milling damage; the argon-ion beam tilt was kept below 2.5° so as to obtain a

relatively large area of observation.

The crystal orientation and grain size of the surface were analyzed using an EBSP system (OIM4; EDAX-TSL Solutions, Tokyo, Japan) in SEM (FE-SEM; JSM 6500F; JEOL). EBSP was performed on the specimen surface at an acceleration voltage of 20 kV and a working distance of 15 mm. The specimens were measured to identify the orientation of the grains, using a step size of 50 nm from an area of 1 μm × 1 μm, to obtain a map of inverse pole figures (IPF map). The grains were defined by a set of measured points whose orientations were close to each other and within a misorientation of 2°.

Surface roughness evaluation

The surface profile and mean surface roughness (Ra) of polished and hydrothermal treated Y-TZP and ATZ pellets were determined using a surface profilometer (Surfcom 2000, Tokyo Seimitsu Co.Ltd., Tokyo, Japan). Five different areas of each specimen were measured and the average Ra of each specimen was estimated.

RESULTS

The degradation of zirconia in a hydrothermal environment and the effect of adding alumina were evaluated by grazing angle XRD analysis. Figure 2 shows the XRD patterns of the Y-TZP surface obtained with the 2θ–θ and grazing angle methods (incident angle = 1°, 2°). The Y-TZP surface was sintered at 1350°C and autoclaved for 3 days in DW. As noted in Eq. (1) and (2), the penetration depth of the incident X-ray into zirconia was varied by changing the incident angle. In the spectra obtained by the 2θ–θ method, strong peaks representing the tetragonal phase were observed, while peaks assigned to the monoclinic phase were not distinct. On the other hand, in the spectra obtained with the grazing angle method (θ = 1° and 2°), clear peaks for monoclinic zirconia were seen. Therefore, the surface transformation of zirconia with hydrothermal treatment could be effectively identified by grazing angle XRD analysis.

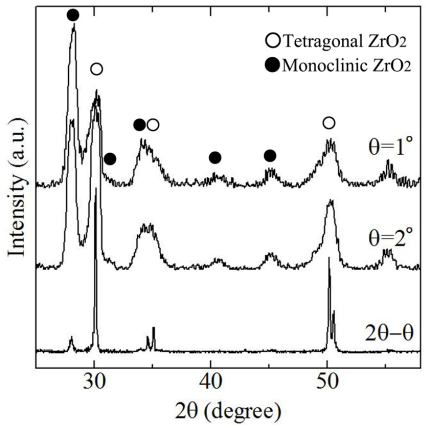

Fig. 2 XRD spectra obtained by the 2θ–θ method and the grazing angle method (1°, 2°). Zirconia was sintered at 1350°C and autoclaved for 3 days.

The monoclinic zirconia contents of the specimens autoclaved for 7 days in DW based on Eq. (3) and (4) for different firing temperatures are shown in Figure 3(a) and (b). With increasing sintering temperature, the monoclinic zirconia content due to hydrothermal treatment increased in both Y-TZP and ATZ. The monoclinic zirconia content of Y-TZP sintered at 1350°C, which is the sintering temperature suggested by the manufacturer, was estimated as 76%, 66%, and 18% at θ = 1°, 2°, and 2θ–θ, respectively [Fig. 3(a)]. The X-ray penetration depth, which is equal to the characterizing depth of XRD, was calculated as 1.2 μm at θ = 1° and 2.3 μm at θ = 2°. Thus, the monoclinic zirconia layer formed on hydrothermal treatment could be assumed to be few micrometers deep. In contrast, ATZ sintered at 1350°C showed less than 40% of monoclinic zirconia content even with θ = 1° [Fig. 3(b)]. Therefore, the thickness of the monoclinic zirconia layer formed on the ATZ surface was estimated to be less than 1 μm.

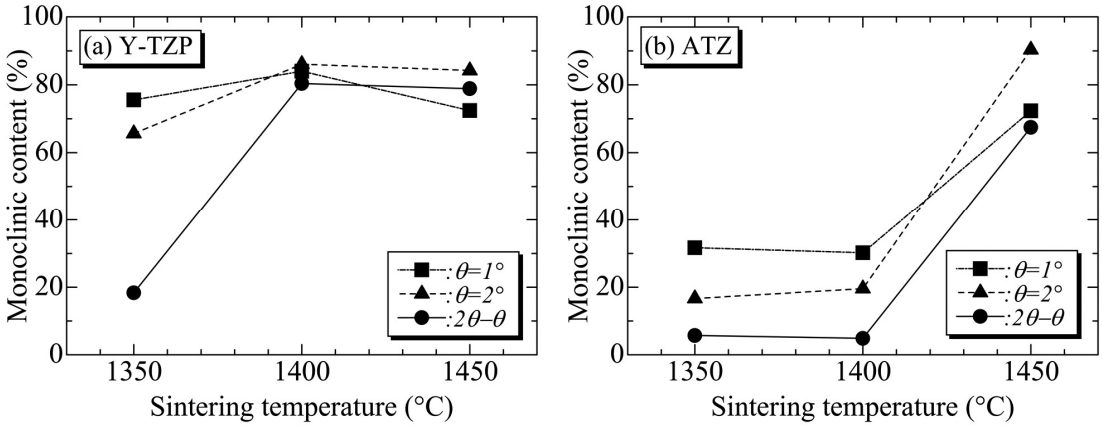

Fig. 3 Monoclinic zirconia contents of (a) Y-TZP and (b) ATZ at different sintering temperatures.

The monoclinic zirconia contents of specimens sintered at 1350°C at different autoclaving times in DW are shown in Figure 4. The monoclinic zirconia content of Y-TZP was greater than that of ATZ for each autoclaving time. At a treatment time of 14 days, the monoclinic zirconia content of Y-TZP was 67 vol%, compared with 37 vol% for ATZ. These results indicate that phase transformation from tetragonal to monoclinic was suppressed by the addition of alumina.

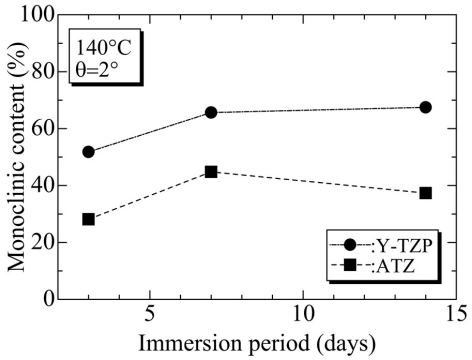

Fig. 4 Monoclinic zirconia contents after different immersion periods.

Figure 5 displays the monoclinic zirconia contents of specimens sintered at 1350°C and autoclaved for 7 days in DW, Hanks, and lactic acid solution. There was no significant difference in monoclinic zirconia content among specimens treated with any of the solutions. We thus believe that the solution used does not affect the hydrothermal degradation of zirconia.

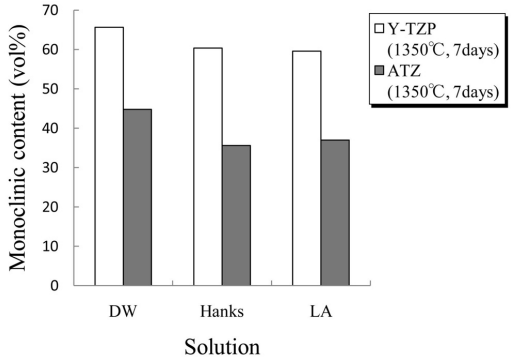

Fig. 5 Monoclinic zirconia contents after autoclaving in different solutions.

Figure 6 shows the typical surface profiles of polished and hydrothermal treated specimens. Y-TZP specimens showed quite flat surface even after the hydrothermal treatment . The average Ra of Y-TZP specimens were less than 0.01μm, which was the detection limit of the profilometer. ATZ specimens showed rough surface compared with Y-TZP. The average Ra of polished and hydrothermal treated ATZ surfaces were estimated as 0.11±0.014 μm and 0.13±0.012 μm, respectively. Thus, both Y-TZP and ATZ showed no significant change in the surface roughness by the hydrothermal treatment.

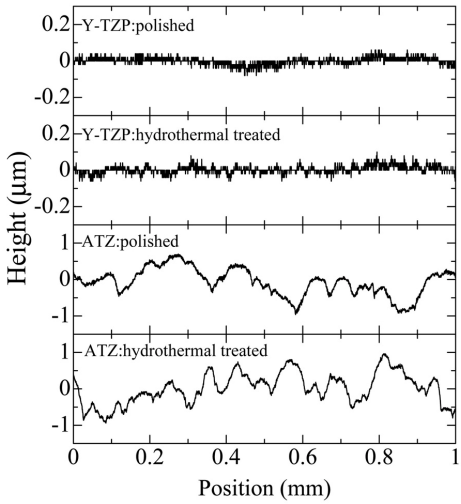

Fig. 6 Typical surface profiles of polished and hydrothermal treated specimens.

Figure 7 shows TEM images of the microstructure of both Y-TZP and ATZ sintered at 1350°C and 1450°C. Y-TZP and ATZ sintered at 1350°C showed similar grain size, while Y-TZP sintered at 1450°C [Fig. 7(c)] showed excessive grain growth (white arrow); the grain growth increased with increasing sintering temperature. ATZ sintered at 1450°C [Fig. 7(d)] also showed grain growth compared with the growth observed when sintering at 1350°C [Fig. 7(b)]. However, grain growth in ATZ was less than that in Y-TZP, and excessive grain growth was not observed. Thus, grain growth was relatively suppressed in ATZ.

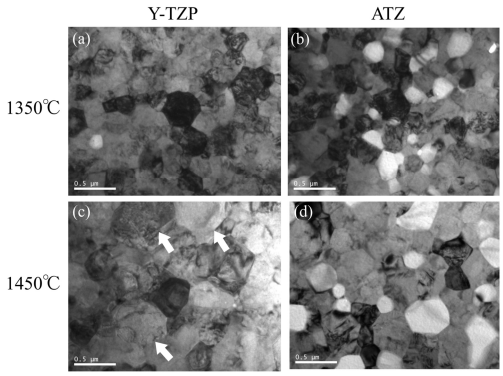

Fig. 7 TEM micrographs of Y-TZP sintered at (a) 1350°C and (c) 1450 °C and ATZ sintered at (b) 1350°C and (d) 1450°C.

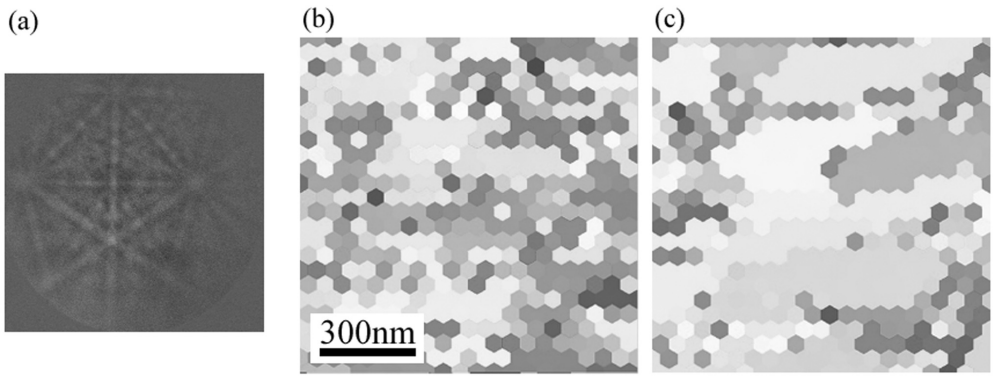

Fig. 8 EBSP image of tetragonal zirconia (a) and IPF mapping images after sintering at 1350°C (b) or 1450°C (c)

Figure 8 shows the EBSP pattern and crystal orientation (IPF) mappings. Figure 8(a) presents an example of the Kikuchi pattern from tetragonal zirconia. The crystallographic orientation of each point on the zirconia surface is represented as orientation maps in Figure 8(b) and (c), which show IPF maps of the Y-TZP surface sintered at 1350°C and 1450°C, respectively. Areas of individual crystal grains are shown in the same color. Y-TZP sintered at the higher temperature [1450°C, Fig. 8(c)] clearly shows larger grain sizes compared with Y-TZP sintered at the lower temperature [1350°C; Fig. 8(b)]. The estimated grain sizes in the IPF maps were in agreement with grain sizes estimated from TEM images [Fig. 7 and Fig. 8(b, c)]. In the case of ATZ, the polished surface was not as perfectly flat as that of Y-TZP because of its inhomogeneity, and therefore, EBSP observation could not be performed.

DISCUSSION

As presented in Figure 2, the monoclinic zirconia layer on the zirconia surface after hydrothermal treatment at 140°C could be clearly detected by grazing angle XRD analysis; therefore, grazing angle XRD analysis was considered appropriate for the evaluation of the monoclinic phase content on zirconia surfaces.

Increasing the sintering temperature markedly increased the monoclinic zirconia content of Y-TZP [Fig. 3(a)]. For Y-TZP sintered at a temperature higher than 1400°C, the monoclinic zirconia content was estimated as approximately 80% using the 2θ–θ method. The penetration depth of X-rays with the 2θ–θ method (at θ = 30°) was calculated as 17.6 μm. This means that more than 10 μm of monoclinic zirconia layer was formed on the Y-TZP surface and that hydrothermal degradation propagated to a greater depth in specimens sintered at the higher temperature. In the case of ATZ [Fig. 3(b)], transformation to the monoclinic phase was suppressed by sintering at 1350°C and 1400°C. Even at 1450°C, the monoclinic zirconia content as estimated by the 2θ–θ method was approximately 60%, which is lower than that for Y-TZP.

Increasing the duration of hydrothermal treatment slightly increased the monoclinic zirconia content, as shown in Figure 4. ATZ always showed a lower monoclinic zirconia content (less than 40%) than Y-TZP up to 14 days of hydrothermal treatment by grazing angle XRD analysis at θ = 2°. This implies that the thickness of the transformed layer would be approximately 1−2 μm. The surface of Y-TZP with hydrothermal treatment for 7 days was quite flat and no significant change was detected from before the treatment. ATZ showed rougher surface because of its high hardness and alumina inclusion. But, the mean roughness (Ra) did not significantly changed by the hydrothermal treatment. Thus, the hydrothermal treatment in the tested specimens would not affect to the surface shape and roughness and also not affected to the geometry of the grazing angle XRD.

Schneider et al.[16] suggested that the temperature dependence of the transformation reaction rate (k) from tetragonal to monoclinic follows the Arrhenius equation:

$$Lnk = -Ea/RT + k_0 \quad (5)$$

where the activation energy Ea is 96.5 ± 4 kJ and the pre-exponential factor k_0 is about 2.7×10^{10} h^{-1}. According to this relation, hydrothermal treatment for 1 week at 140°C would correspond to more than 200 years at 37°C. Therefore, ordinary intra-oral use of ATZ would result in hydrothermal degradation to just less than few micrometers below the surface, which would not affect the properties of ATZ. Thus, suppression of hydrothermal degradation and phase transformation by addition of alumina to zirconia was confirmed by grazing angle XRD analysis.

The TEM and EBSP images (Figs 7 and 8) reveal the excessive grain growth in Y-TZP and ATZ as the sintering temperature increased from 1350℃ to 1450℃. The grain sizes were similar for Y-TZP and ATZ sintered at 1350℃, but most grains in Y-TZP showed excessive growth with sintering at 1450℃. ATZ also showed grain growth, but small grains continued to be present and excessive grain growth was also slightly suppressed compared with Y-TZP. Increasing the sintering temperature caused greater hydrothermal degradation, as shown in Fig. 7(a) and Fig. 8(c). Thus, the hydrothermal degradation of zirconia appears to be related to grain size and structure.

CONCLUSION

The increase in phase transformation of the zirconia surface with hydrothermal degradation in Y-TZP and ATZ could be clearly observed by grazing angle XRD analysis. ATZ showed a lesser degree of phase transformation to the monoclinic phase, and hydrothermal treatment and transformation were suggested to occur within few micrometers from the surface. The monoclinic phase content of ATZ with higher sintering temperatures was also lower than that of Y-TZP, indicating that the presence of alumina in ATZ is effective in suppressing hydrothermal degradation. From the TEM and EBSP observations, grain growth in ATZ was slightly suppressed compared with that in Y-TZP at higher sintering temperatures. These results suggest that the addition of alumina to zirconia for the suppression of hydrothermal degradation is effective and that a relationship exists between hydrothermal degradation and grain growth.

ACKNOWLEDGMENTS

This work was supported by Grant-in-Aid for Challenging Exploratory Research No. 21659449 from the Ministry of Education, Culture, Sports, Science and Technology, Japan.

REFERENCES

1) Garvie RC, Hannink RH, Pascoe RT. Ceramic steel? Nature 1975; 258: 703-704.

2) Hannink RH, Kelly PM, Muddle BC. Transformation toughening in zirconia-containing ceramics. J Am Ceram Soc 2000; 83: 461-487.

3) Piconi C, Maccauro G. Zirconia as a ceramic biomaterial. Biomaterials 1999; 20: 1-25.

4) Chevalier J, Gremillard L, Virkar AV, Clarke DR. The tetragonal-monoclinic transformation in zirconia: lessons learned and future trends. J Am Ceram Soc 2009; 92: 1901-1920.

5) Raigrodski AJ. Contemporary materials and technologies for all-ceramic fixed partial dentures: a review of the literature. J Prosthet Dent 2004; 92: 557-562.

6) Tinschert J, Zwez D, Marx R, Anusavice KJ. Structural reliability of alumina-, feldspar-, leucite-, mica- and zirconia-based ceramics. J Dent 2000; 28: 529-535.

7) Seiji B. Reliability and properties of core materials for all-ceramic dental restorations. Japanese Dental Science Review 2008; 44: 3-21.

8) Moser EM, Keller BA, Lienemann P, Hug P. Surface analytical study of hydrothermally treated zirconia ceramics. Fresenius J Anal Chem 1993; 346: 255-260.

9) Chevalier J, Cales B, Drouin JM. Low-temperature aging of Y-TZP ceramics. J Am Ceram Soc 1999; 82: 2150-2154.

10) Salehi SA, Vanmeensel K, Swarnakar AK, Van der Biest O, Vleugels J. Hydrothermal stability of mixed stabilized tetragonal (Y, Nd)-ZrO_2 ceramics. Journal of Alloys and Compounds 2010; 495: 556-560.

11) Seiji B, Yasuhiko S, Hideo N, Masahiro N. Fracture toughness of dental zirconia before and after autoclaving. J Ceram Soc Japan 2010; 118: 406-409.

12) Eichler J, Rodel J, Ulrich E, Mark H. Effect of grain size on mechanical properties of submicrometer 3Y-TZP: fracture strength and hydrothermal degradation. J Am Ceram Soc 2007; 90: 2830-2836.

13) Lin JD, Duh JG. Crystallite size and microstrain of thermally aged low-ceria-and low-yttria-doped zirconia. J Am ceram Soc 1998; 81: 853-860.

14) Nevarez-Rascon A, Aguilar-Elguezabal A, Orrantia E, Bocanegra-Bernal MH. On the wide range of mechanical properties of ZTA and ATZ based dental ceramic composites by varying the Al_2O_3 and ZrO_2 content. Int Journal of Refractory Metals & Hard Materials 2009; 27: 962-970.

15) Kim DJ, Lee MH, Lee DY, Han JS. Mechanical properties, phase stability, and biocompatibility of (Y, Nd)-TZP/Al_2O_3 composite abutments for dental implant. J Biomed Mater Res 2000; 53: 438-443.

16) Schneider J, Begand S, Kriegel R, Kaps C, Glien W, Oberbach T. Low-temperature aging behavior of alumina-toughened zirconia. J Am Soc 2008; 91: 3613-3618.

17) Rigaku Co, XRD handbook. 4th ed. Rigaku Co: Tokyo, Japan; 2003. p. 107-109.

18) Hideo T, Masahiro Y, Shigeyuki S. Calibration curve for quantitative analysis of monoclinic-tetragonal ZrO_2 system by X-ray diffraction. J Am Soc 1984; 67: C119-C121.